

## Sign-time distributions for interface growth

Z. Toroczkai,<sup>1,2</sup> T. J. Newman,<sup>1</sup> and S. Das Sarma<sup>2</sup>

<sup>1</sup>*Department of Physics, Virginia Polytechnic Institute and State University, Blacksburg Virginia 24061*

<sup>2</sup>*Department of Physics, University of Maryland, College Park, Maryland 20742*

(Received 27 October 1998; revised manuscript received 11 May 1999)

We apply the recently introduced distribution of sign-times (DST) to nonequilibrium interface growth dynamics. We are able to treat within a unified picture the persistence properties of a large class of relaxational and noisy linear growth processes, and prove the existence of a nontrivial scaling relation. A critical dimension is found, relating to the persistence properties of these systems. We also illustrate, by means of numerical simulations, the different types of DST to be expected in both linear and nonlinear growth mechanisms. [S1063-651X(99)50608-9]

PACS number(s): 05.40.-a, 05.70.Ln, 82.20.Mj

The notion of persistence, or the statistics of first passage events, has been a powerful conceptual tool in studying stochastic non-Markovian processes in many research areas of physics, engineering, statistics, and applied mathematics. In this Rapid Communication we apply a persistence-related concept, the distribution of sign-times, or DST (defined below), to the problem of kinetic surface roughening in non-equilibrium interface growth dynamics [1]. We believe that the ideas, described in this paper, could become an extremely useful conceptual and practical tool in characterizing surface growth dynamics, rivaling the dynamic scaling ideas currently used in studying kinetic surface roughening. Depending on the specific issues of interest, our proposed DST technique may actually be more powerful and informative than the currently fashionable dynamical/roughness/growth exponent based characterization of dynamical surface morphologies.

One of the main themes in the theory of nonequilibrium interfaces is grouping the interface roughening phenomena within “universality classes”. This classification of scenarios is based on calculating the dynamic scaling properties of the surface correlation function [1]. On the other hand, in non-equilibrium interface growth experiments, one might also be interested in morphology stability issues which can in fact be formulated as first passage type questions: what is the probability that a mound (or crevice) will survive as a mound (crevice) for a given period of time  $t$ ? How does this probability decay in time, etc.? These type of questions, however, are not simply delineated by such a correlation function.

Another open theoretical problem is to establish a correspondence between discrete solid-on-solid (SOS) models and continuum Langevin equations beyond the equality of exponents. For example, based on structure factor measurements, the authors in Ref. [2] claim that the SOS model they introduced does not only belong to the same universality class as the noisy Mullins equation but it is described *exactly* by it. Our approach proposed in the present Rapid Communication (which is *not* based on direct measurement of the correlation function) supports that claim.

It would be useful, therefore, to study statistical quantities that are directly sensitive to the structural and morphological properties of interfaces (e.g., formation of mounds) and to the dynamics of these structures (e.g., coarsening). In this

Rapid Communication, we propose that such information may be inferred from the DST, which has recently been introduced in the context of the persistence properties of simple coarsening systems and the diffusion equation [3,4]. First passage time or persistence problems have been the focus of intensive research for the past few years, producing a series of analytic and numerical results with applications to the Ising and Potts models [5], the diffusion equation [6], phase ordering [7], interface kinetics [8], etc. and experiments on liquid crystals and soap froths (see the references in [6]). The central issue of persistence concerns the probability of an event *never* occurring (up to a certain time  $t$ ). It is very restrictive by definition, and good statistics from numerics or experiments may be extremely hard to obtain. The recently introduced [3,4] DST is practically more accessible, and as a limiting case produces the persistence probability.

The DST is essentially a histogram performed on the sign of the fluctuations and simply measures the probability of the fluctuations having been in the positive domain for a total time  $\tau$  in the given time  $t$  of the process. Obviously for  $\tau = t$  we obtain the usual persistence probability, which we denote by  $P_+(t)$ , and for  $\tau=0$  we obtain the probability of the fluctuations having *never* been in the positive domain, i.e. to have been *always* in the negative domain,  $P_-(t)$ . The distinction between the persistence of fluctuations in the positive domain and in the negative domain becomes important in the case of nonlinear models [9]. We shall refer to these as “positive” and “negative” persistence, respectively.

The sign-time for an interface on a  $d$ -dimensional substrate is the stochastic variable defined by

$$T(\mathbf{x}, t) = \int_0^t dt' H(h(\mathbf{x}, t')), \quad (1)$$

where  $H$  is the Heaviside step function and  $h(\mathbf{x}, t)$  is the height of the interface measured with respect to the average height. Since  $h$  is a random variable (due to its coupling to the noise) the sign-time will be described by a probability distribution, the DST. For a system with translation invariance, the statistics of  $\tau$  will not depend on the location  $\mathbf{x}$ , and so the DST may be written as

$$S(\tau, t) = \langle \delta(\tau - T(\mathbf{0}, t)) \rangle, \quad (2)$$

where  $\langle \cdot \rangle$  indicates the average over the noise. Some properties of  $S$  are (i) it is defined on the interval  $0 \leq \tau/t \leq 1$ ; (ii) for interface growth with  $h \rightarrow -h$  symmetry,  $S$  will be symmetric about  $\tau/t = 1/2$ ; (iii) the tails of the distribution give the persistence probabilities:  $P_-(t) = \int_0^\epsilon d\tau S(\tau, t)$  and  $P_+(t) = \int_0^\epsilon d\tau S(t - \tau, t)$ , where  $\epsilon \ll t$  is a microscopic time scale (of the order of the fastest temporal scale in the interface dynamics). These probabilities are expected to have a power law decay, defining the corresponding persistence exponents  $\theta_\pm$ :  $P_\pm(t) \sim (\epsilon/t)^{\theta_\pm}$ , and (iv) the shape of  $S$  contains information about whether the growth is rare event dominated or not.

In the spirit of Ref. [8] we first consider the following class of stochastic linear equations:

$$\partial_t h = -\nu(-\nabla^2)^{z/2} h + \xi, \quad (3)$$

with flat  $[h(\mathbf{x}, 0) = 0]$  initial condition, where  $\xi$  is a general noise term that may represent the ‘‘pure deterministic’’ case via the choice  $\xi(\mathbf{x}, t) = \delta(t)\eta(\mathbf{x}, t)$  or the regular ‘‘noisy’’ case with  $\xi(\mathbf{x}, t) = \eta(\mathbf{x}, t)$ , where  $\eta$  is a Gaussian-distributed noise possibly with spatial correlations. We consider the following three choices for  $\eta$ : (1) white noise with correlator  $\langle \eta(\mathbf{x}, t)\eta(\mathbf{x}', t') \rangle = 2D\delta(\mathbf{x} - \mathbf{x}')\delta(t - t')$ , (2) volume conserving noise  $\langle \eta(\mathbf{x}, t)\eta(\mathbf{x}', t') \rangle = -2D\nabla^2\delta(\mathbf{x} - \mathbf{x}')\delta(t - t')$ , and (3) long range spatially correlated noise  $\langle \eta(\mathbf{x}, t)\eta(\mathbf{x}', t') \rangle = 2D|\mathbf{x} - \mathbf{x}'|^{\rho-d}\delta(t - t')$ ,  $\rho < d$ . For example, the Edwards-Wilkinson (EW) model may be recovered by setting  $z = 2$  in Eq. (3), and by applying white noise; likewise, the noisy Mullins equation corresponds to setting  $z = 4$  [1]. We write Eq. (2) through the higher moments of DST as

$$S_d^{(z)}(\tau, t) = \sum_{n=0}^{\infty} \int_{-\infty}^{\infty} \frac{d\omega}{2\pi} e^{i\omega\tau} \frac{(-i\omega)^n}{n!} \langle [T_d^{(z)}(\mathbf{0}, t)]^n \rangle, \quad (4)$$

where we have introduced a frequency representation of the  $\delta$  function, and expanded in powers of the sign-time  $T_d^z$ . We shall enter into no technical details here on how to proceed with calculating the moments of the DST. We present only the final form that we obtained for the  $n^{\text{th}}$  order moment normalized by  $t^n$  [ $\mu_n \equiv \langle (\tau/t)^n \rangle$ ]

$$\mu_n = \prod_{k=1}^n \int_0^1 \frac{da_k}{2\pi} \int_{-\infty}^{\infty} \frac{d\sigma_k}{\epsilon_k + i\sigma_k} \exp\left(-\sum_{j,l} \sigma_j \sigma_l \kappa(a_j, a_l)\right), \quad (5)$$

where the limits of  $\epsilon_k \rightarrow 0^+$  are to be taken, and

$$\kappa(x, y) = \begin{cases} (x+y)^{-\gamma}, & \text{deterministic case} \\ \int_0^{\min(x,y)} du (x+y-2u)^{-\gamma}, & \text{noisy case,} \end{cases} \quad (6)$$

with  $0 \leq x, y \leq 1$ , and  $\gamma$  being given by (1)  $\gamma = d/z$  for the deterministic case and for white noise, (2)  $\gamma = (d+2)/z$  for volume conserving noise, and (3)  $\gamma = (d-\rho)/z$  for long-

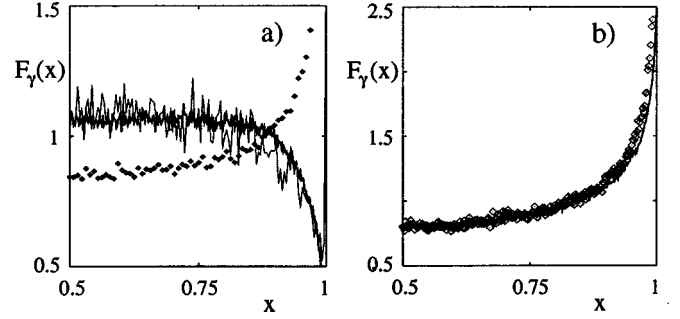


FIG. 1. DST’s for (a)  $\{1,2\}$  (thick line) at  $t = 0.25 \times (2 \times 10^3)$  obtained on a grid of  $L = 2048$  sites and averaged over  $2 \times 10^3$  runs;  $\{2,4\}$  at  $t = 0.01 \times 256$  (dots), and  $t = 0.01 \times 4096$  (thin line), on a grid of  $1024 \times 1024$  shown for a single run. (b) the SOS large curvature model (diamonds) on a lattice of  $L = 10^4$  at 8192 steps, averaged over 100 runs; and for  $\{1,4\}$  measured on a grid of  $L = 2048$  sites at  $t = 0.05 \times (2 \times 10^3)$ , and averaged over  $2 \times 10^3$  runs (continuous line). Due to the symmetry property (ii) the DST’s are shown only in the half range  $x \in [0.5, 1]$ .

range correlated noise. We make the following observations from Eqs. (4)–(6). First, the DST obeys the exact scaling form

$$S_d^{(z)}(\tau, t) = \frac{1}{t} F_\gamma\left(\frac{\tau}{t}\right), \quad 0 \leq \tau \leq t, \quad (7)$$

for all values of  $t$  ( $\mu_n$  is  $t$  independent). Second, the ‘‘material parameters’’  $\nu$  and  $D$  do not appear in the DST. Third, the three numbers  $(d, z, \rho)$  appear in the DST (for any  $t$ ) only through their combination in  $\gamma = \gamma(d, z, \rho)$ . Thus, the persistence exponents (which are contained within the DST) will also only depend on  $d$ ,  $z$ , and  $\rho$  through the exponent  $\gamma$ . [This appears to be implicitly understood in Ref. [8], where persistence is measured as a function of the growth exponent  $\beta = \max(0, (1 - \gamma)/2)$ .] A similar scaling property for the persistence exponents is also true for the deterministic case.

For simplicity of the notation, instead of  $S_d^{(z)}(\tau, t)$  (and  $\theta_d^{(z)}$ ) we will use  $S_\gamma(\tau, t)$  (and  $\theta_\gamma$ ). Let us consider as an example the generic case of white noise, for which  $\gamma = d/z$ . According to the above, for any model for which, e.g.,  $d/z = 0.5$ , the DST (and thus the persistence properties) will be identical to that for the EW model in one dimension. We compared the numerically obtained DST’s for  $\{1,2\}$  (meaning  $d=1, z=2$ ) and  $\{2,4\}$ . According to the above, one should observe identical DST’s. The  $\{1,2\}$  DST was measured using a standard discretization scheme, see Fig. 1(a). The numerical integration of the case  $\{2,4\}$  is less straightforward. We used the simplest discrete scheme for modeling the operator  $\nabla^4$  in  $d=2$ , as more sophisticated schemes were actually less stable under the influence of additive white noise. A very small integration time step of  $\delta t = 0.01$  was used to ensure stability. We observed a long transient in which the DST was actually concave, in contrast to the convex DST for the case  $\{1,2\}$  ( $d=1$  EW model). After  $10^3$  iterations the DST began to turn over, and eventually settled into a convex shape, closely matching the  $\{1,2\}$  DST. This illustrates the sensitivity of the DST to lattice effects, which may be a very useful property if one is investigating physics

which is itself sensitive to the underlying lattice. In Fig. 1(b) we show the DST's obtained from numerical integration of the case  $\{1,4\}$  (the  $d=1$  noisy Mullins equation) and numerical simulation of the SOS large curvature model [2]. These two models are expected to have very similar properties, and indeed their DST's are almost indistinguishable.

It follows from Eqs. (4)–(6) that the knowledge of the second moment  $\mu_2$  *uniquely* determines the value of  $\gamma$ , and therefore also  $z$  (in a given dimensionality). It is possible to evaluate analytically the second moment  $\mu_2$ . We find  $\mu_2 = 1/2 - G(\gamma)$ , where for the deterministic case

$$G(\gamma) = \frac{\gamma}{4\pi} \int_0^1 da \frac{1-a}{1+a} \left[ \left( \frac{1+a}{2a^{1/2}} \right)^{2\gamma} - 1 \right]^{-1/2}, \quad (8)$$

and for the noisy case

$$G(\gamma) = \frac{1}{2\pi} \int_0^1 da \times \arctan \sqrt{\frac{(4a)^{1-\gamma}}{[(1+a)^{1-\gamma} - (1-a)^{1-\gamma}]^2}}. \quad (9)$$

The second moment in both cases is a monotonic function of  $\gamma$  and therefore the knowledge of one determines the other; a property useful in deciding whether a measured DST can indeed be described by a process like Eq. (3). For example, one may obtain from numerical or experimental measurements a symmetric DST, from which one may compute  $\mu_2$ . One can *test* therefore if the process generating the measured DST can be described by Eq. (3): one determines  $z$  using the above procedure, and then simulates Eq. (3) with the corresponding value of  $\gamma$ , thus generating a new DST. If the two DST's are very close or coincide, then the assumption that the physical process may be modeled by Eq. (3) is valid, just as in the SOS large curvature model case, shown in Fig. 1(b). Note, that this procedure also requires an assumption about the type of noise.

The integral in Eq. (6) is divergent for  $\gamma > 1$  at  $x = y$ . Introducing a microscopic lattice cut-off, the DST can be calculated [10] to give a Dirac  $\delta$  function centered around  $\tau = t/2$

$$S_\gamma(\tau, t) = \frac{1}{t} \delta\left(\frac{1}{2} - \frac{\tau}{t}\right), \quad \text{for any } \gamma > 1. \quad (10)$$

It is a well known result [1] that for Eq. (3),  $d = d_u = z$  is an upper critical dimension and separates interfaces that are asymptotically rough from those which are asymptotically smooth. Thus, the fact that for dimensions above  $z$  there is no roughening, is reflected by a  $\delta$  function DST, i.e., *all* points of the interface will spend exactly half of their time above the mean height. The persistence exponent in this case is not really defined, since the persistence probability is zero. In a lattice model, one would expect corrections to scaling to the above result, and for the persistence probability to decay exponentially with time. When approaching  $\gamma_u \equiv d_u/z = 1$  from below, the persistence exponent diverges;  $\gamma = \gamma_u$  being a marginal case for which no numeric or analytic results have been produced yet (on persistence properties). It is precisely

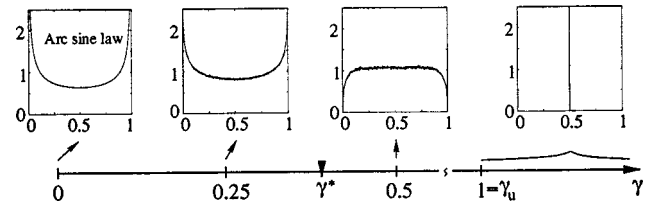


FIG. 2. Behavior of DST as a function of  $\gamma$  for Eq. (3), with white noise. Each inset shows the function  $F_\gamma(x)$  vs  $x$ . For  $\gamma = 0.25$  and  $\gamma = 0.5$  we simulated the Langevin equation with white noise in one dimension at  $z = 4$  and  $z = 2$ , respectively. For  $z = 2$  the simulation parameters were the same as for the thick line in Fig. 1(a) and for  $z = 4$  they were the same as for the continuous line in Fig. 1(b).

the case of the two dimensional EW equation with white noise. Note that the EW equation in any integer dimension ( $d \geq 1$ ) with volume conserving noise is in the smooth phase, and would therefore have a  $\delta$  function DST ( $\gamma = 1 + d/2$ ), with the persistence exponent undefined (or formally infinite).

From the scaling relation (7) one can infer the existence of a new critical “dimension”  $\gamma^*$  both for the deterministic and noisy cases: since the tails of DST give the persistence probability, which has a power law decay ( $P_\pm \sim t^{-\theta}$ ), the scaling function  $F_\gamma$  must obey the behavior  $F_\gamma(x) \sim x^{\theta-1}$ , for  $x \ll 1$ , and  $1-x \ll 1$  in order that Eq. (7) be satisfied. For  $\theta < 1$  the DST has integrably divergent tails while for  $\theta > 1$  the tails vanish (as  $x^{\theta-1}$ ). In the former case the sites are more likely to be found in a positive or negative persistent state (i.e., with a height that did not change sign at all), while in the latter case persistent sites will be an absolute minority (with vanishing measure as  $t \rightarrow \infty$ ). Since  $\theta_\gamma$  is a monotonically increasing function of  $\gamma$  the equation  $\theta_\gamma = 1$  will be satisfied at a unique value of  $\gamma^*$ . At this value  $F_{\gamma^*}$  is flat at the tails: it neither falls to zero nor diverges. This shows that the value of  $\theta_{\gamma^*} \equiv \theta_{d^*}^{(z)} = 1$  is special. It is possible that  $F_{\gamma^*}$  can still have some structure around  $\tau/t = 1/2$ , but the simplest possibility is that it is a top-hat function. In this case  $\mu_2 = 1/3$ , and therefore  $\gamma^*$  can be calculated after (numerically) inverting  $G(\gamma) = 1/6$ , using Eqs. (8) and (9). For the deterministic case one obtains  $\gamma^* = 17.983\dots$ , and for the noisy case  $\gamma^* = 0.438\dots$ . In fact, exact bounds exist [8] for the relation between  $\beta$  and  $\theta$  from which we find that  $\gamma^* \leq 0.36\dots$ . Therefore our approximate value of  $\gamma^*$  lies above the bound, which implies that at criticality (namely,  $\theta = 1$ ), the DST, although having flat tails, still has nontrivial structure around  $\tau = t/2$ . For the noisy case, our numerical simulations are compatible with  $0.25 < \gamma^* < 0.5$ , as can be seen from Fig. 2. It is interesting to note that the permanent presence of noise “brings down” this critical  $\gamma^*$  to a sub-unitary value as compared to the deterministic case.

The DST for  $\gamma = 0$  is exactly known, and is called the “arcsine law” in the mathematical literature [11]:  $F_0(x) = 1/[\pi \sqrt{x(1-x)}]$ , which can also be derived from Eqs. (4)–(6) presenting an alternative to this venerable old problem. Figure 2 summarizes our findings on the different regimes for the DST of the noisy case of Eq. (3) with the two critical “dimensionalities”  $\gamma^*$  and  $\gamma_u$ .

We shall now present and briefly discuss the numerically obtained DST's for two nonlinear systems: (1) the one di-

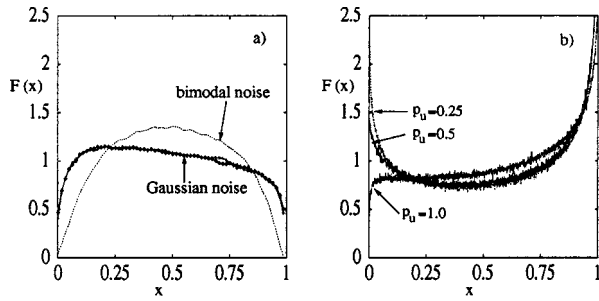


FIG. 3. (a) DST for the  $d=1$  KPZ equation with white noise at  $t=512$ ,  $t=1024$  and for bimodal noise at  $t=2048$ . (b) DST for the SOS DT model with Schwoebel barriers at  $t=10^3$  steps shown for three different values of the parameter  $p_u$ , which is the probability for an atom to attach to a lower step. The system size was  $L=100$ , and the averaging was made over  $2 \times 10^4$  runs for each curve.

dimensional KPZ equation, and (2) the Das Sarma-Tamborenea (DT) SOS model with Schwoebel barriers. Figure 3(a) shows the KPZ case at different times and with two different noise types (Gaussian and bimodal), using the discretization scheme introduced in Ref. [12]. For the case of Gaussian noise one can see that the DST satisfies the general scaling form (7) but with an asymmetric scaling function  $F(x)$  since the  $h \rightarrow -h$  symmetry is broken, reflecting the nonlinear character of the KPZ equation. The DST for the case of bimodal noise has a different shape to that for Gaussian noise, which was still evolving for the largest times we observed ( $t \sim 10^4$ ), indicating either very long crossover

times, or else a more complicated scaling form. Figure 3(b) shows the DST obtained numerically from the DT model with Schwoebel barriers [13]. This system is highly nonlinear, exhibits mound-formation and coarsening. The DST mirrors all these morphological and structural characteristics. Nonlinearity is obvious from the asymmetric shape. The right end of the curve has the highest value, meaning that the sites are most likely to be found in a positive persistent state, i.e., they belong to structures that stayed above the mean height all the time, namely, *stable mounds*. On the contrary, the left end, when compared to the right one, is in the minority, showing that the *stable crevices*, or *valleys* will contain only a small fraction of the sites, which points to a mounded morphology with high skewness. The fact that a site has a small probability to survive for a long time in a crevice, means that the valleys tend to disappear during time-evolution, i.e., there must be *coarsening*. This shows the intimate connection between the coarsening and persistence properties of an interface morphology, which is the topic of a separate, forthcoming publication.

In summary, the DST proves to be very sensitive to the details of the morphological dynamics, and can provide crucial information on the nonequilibrium interface fluctuations.

The authors are grateful to R. Desei, T. Einstein, P. Punyindu, B. Schittmann, R.K.P. Zia, and E.D. Williams for interesting discussions. Financial support is acknowledged from the Materials Research Division of the National Science Foundation (T.J.N. and Z.T.), MRSEC (Z.T. and S.D.S.), and from the Hungarian Science Foundation, T17493 and T19483 (Z.T.).

- 
- [1] J. Krug, *Adv. Phys.* **46**, 139 (1997).  
 [2] J. M. Kim and S. Das Sarma, *Phys. Rev. Lett.* **72**, 2903 (1994).  
 [3] I. Dornic and C. Godreche, *J. Phys. A* **31**, 5413 (1998).  
 [4] T. J. Newman and Z. Toroczkai, *Phys. Rev. E* **58**, R2685 (1998).  
 [5] B. Derrida *et al.*, *Phys. Rev. Lett.* **75**, 751 (1995).  
 [6] S. N. Majumdar *et al.*, *Phys. Rev. Lett.* **77**, 2867 (1996); B. Derrida *et al.*, *ibid.* **77**, 2871 (1996); S. N. Majumdar and A. J. Bray, *ibid.* **81**, 2626 (1998).  
 [7] B. P. Lee *et al.*, *Phys. Rev. Lett.* **79**, 4842 (1997).  
 [8] J. Krug *et al.*, *Phys. Rev. E* **56**, 2702 (1997).  
 [9] H. Kallabis and J. Krug, e-print cond-mat/9809241.  
 [10] T. J. Newman *et al.* (unpublished).  
 [11] P. L evy, *Processus Stochastiques et Mouvement Brownien* (Gauthier-Villars, Paris, 1948).  
 [12] T. J. Newman and M. R. Swift, *Phys. Rev. Lett.* **79**, 2261 (1997).  
 [13] S. Das Sarma and P. Punyindu, e-print cond-mat/9801313; S. Das Sarma and P. Tamborenea, *Phys. Rev. Lett.* **66**, 325 (1991).